Journal of Metals, Materials and Minerals, 34(3), 2083, 2024

Fabrication and characterization of zinc anode on nickel conductive cloth for high-performance zinc ion battery applications

Tanapoom MAWINTORN[1], Kittima LOLUPIMAN[2], Napat KIATWISARNKIJ[3], Pattaraporn WOOTTAPANIT[2], Manickavasakam KARNAN[2,*], Suwimon SANEEWONG NA AYUTTAYA[4], Xinyu ZHANG[5], Panyawat WANGYAO[3,*] and Jiaqian QIN[2,*]

[1] *Defense Engineering and Technology, Faculty of Engineering, Chulalongkorn University, Bangkok 10330, Thailand*
[2] *Center of Excellence in Responsive Wearable Materials, Metallurgy and Materials Science Research Institute, Chulalongkorn University, Bangkok, 10330, Thailand*
[3] *Metallurgical Engineering Department, Faculty of Engineering, Chulalongkorn University, Bangkok 10330, Thailand*
[4] *Department of Mechanical Engineering, Chulachomklao Royal Military Academy, Nakhon Nayok 26000, Thailand*
[5] *State Key Laboratory of Metastable Materials Science and Technology, Yanshan University, Qinhuangdao 066004, P. R. China*

***Corresponding author e-mail**: karnan1051@gmail.com, Jiaqian.Q@chula.ac.th, Panyawat.W @chula.ac.th

Received date:
11 June 2024
Revised date:
3 July 2024
Accepted date:
12 July 2024

Keywords:
Zn-ion batteries;
Electroless nickel;
Cotton;
Flexible zinc-ion battery anodes

Abstract

The development of advanced materials for energy storage is critical to addressing global energy challenges. Zinc-ion batteries offer a promising solution due to their safety, cost-effectiveness, and environmental friendliness. In this study, we enhanced the conductivity of cotton by coating it with electroless nickel, followed by zinc electroplating, to create a flexible material suitable for zinc-ion battery applications. Cotton was coated with electroless nickel at temperatures ranging from 40°C to 60°C for 1 min to 13 min. Subsequently, zinc electroplating was performed with current densities of 0.02 A·cm^{-2} for 60 min, 0.03 A·cm^{-2} for 40 min, and 0.04 A·cm^{-2} for 30 min. The resulting material was used to assemble a battery with an $(NH_4)_2V_{10}O_{25}\cdot 8H_2O$ (NVO) cathode. The Scanning Electron Microscope (SEM) confirms the electroless nickel-coating on cotton fabric at 50°C for 9 min resulted in a low electrical resistance of 15 ohms. Subsequent zinc electroplating at 0.03 A·cm^{-2} for 40 min fully interconnected zinc particles. This research demonstrates the significant potential for further development in the field of textile materials for electrical conductivity. It also makes it possible to incorporate materials like silk cloth and other materials in battery components, which will help build more sustainable energy sources in the future.

1. Introduction

The fascinating aspect lies in the continuous evolution of energy storage technology, which has led to the widespread reliance on electrical energy for various everyday devices [1-5]. This energy is primarily sourced from batteries, which have seen remarkable advancements, focusing on reducing weight and increasing flexibility [6]. Due to these technical advancements, batteries can now be used for wearable, compact, and easily accessible devices. Batteries are commonly categorized as either primary, which is non-rechargeable, or secondary, which is rechargeable [7-11]. Lithium-ion batteries (LIBs), classified as secondary batteries, are widely favored for their exceptional energy density and recharging ability [12]. Currently, researchers focussing on various alternative elements like sodium, potassium, aluminum, and zinc for battery production, with a notable focus on zinc-ion batteries (ZIBs) as a promising advancement in energy storage technology. Zinc-based batteries tend to be more affordable than lithium-based ones because zinc is more plentiful and less costly than lithium [13,14]. Moreover, these batteries feature superior safety characteristics, being less likely to overheat or catch fire compared to lithium-ion batteries. It perceives them as a compelling option for applications where safety is paramount, such as in electric vehicles, portable devices, and large-scale energy storage systems [15]. Furthermore, ongoing research is centered on enhancing the energy density and longevity of zinc-based batteries through the meticulous design and modification of the working electrodes, rendering them appropriate for wearable and flexible battery applications.

To create flexible batteries for wearable applications, researchers have developed various preparation methods [16-19]. These methods include brush coating, immersion followed by drying, using carbon cloth, and non-electroplating techniques[20,21]. Each approach has its unique technique. Among these, one of the simpler and more scalable methods is electroless plating[22-25]. In this study, we will investigate the development of flexible zinc-ion batteries, utilizing cotton fabric as the primary surface material. The selection of cotton is based on its natural origin, cost-effectiveness, and lightweight characteristics, making it an ideal candidate for the fabrication of flexible energy storage devices. Due to cotton fabric's inherent lack of

electrical conductivity, our approach will involve the application of electroless nickel (Ni) coating to enhance its conductivity, as supported by existing literature [26,27]. Subsequently, electroplating techniques will be utilized to fabricate the anode, laying the groundwork for the assembly of zinc-ion batteries [28]. The efficacy and feasibility of this innovative approach will be systematically evaluated, with a focus on its potential for practical implementation in flexible electronic devices.

2. Experimental

2.1 Electroless nickel-coating process for cotton fabric

The cotton underwent an initial cleaning process when it was immersed in a 100 $g \cdot L^{-1}$ NaOH solution at 50°C for 10 min, followed by two rinses with deionized water at room temperature. The cotton was then sensitized for 7 min in a solution of 10 $g \cdot L^{-1}$ $SnCl_2$ and 30 $mg \cdot L^{-1}$ HCl, activated in a solution of 0.1 $g \cdot L^{-1}$ $PdCl_2$ and 30 $mg \cdot L^{-1}$ HCl, and the sensitized electrodes were dried. The fabric pieces were then submerged in a nickel plating solution, which consisted of $NiSO_4 \cdot 6H_2O$ (0.17 $mol \cdot L^{-1}$), $(NH_4)_2SO_4$ (0.23 $mol \cdot L^{-1}$), $Na_3C_6H_5O_7$ (0.16 $mol \cdot L^{-1}$) and the pH was adjusted to 8 with NaOH. $NaH_2PO_2 \cdot H_2O$ was also added to the solution with a concentration of 0.25 $mol \cdot L^{-1}$, and the fabric was treated for 1 min to 13 min at 40°C to 60°C. Subsequently, resistance measurements were taken at nine 1 cm intervals along the fabric and averaged.

2.2 Zinc electroplating process

The electroplating bath is composed of $ZnSO_4 \cdot 7 \cdot H_2O$ at a concentration of 200 $g \cdot L^{-1}$, Na_2SO_4 at 80 $g \cdot L^{-1}$, NaCl at 40 $g \cdot L^{-1}$, H_3BO_3 at 16 $g \cdot L^{-1}$, and a total volume of 1 L of deionized water [29]. Electroplating is carried out using precise current densities: 0.02 $A \cdot cm^{-2}$ for 60 min, followed by 0.03 $A \cdot cm^{-2}$ for 40 min, and finally 0.04 $A \cdot cm^{-2}$ for 30 min. Following the electroplating process, the plated workpiece undergoes annealing at a temperature of 80°C for 12 h. Once all the procedures have been completed, the finished product is prepared to be used as the anode in a zinc-ion battery.

2.3 Physical characteristics

The surface characterization of the sample was examined by using scanning electron microscopy (SEM, Hitachi S4800). The calculation of electrolyte absorption was performed using the equation: [30] uptake = (Wa – Wb)/Wb × 100%, where Wb and Wa represent the weight of separators before and after being immersed in the electrolyte for 1 h.

2.4 Electrochemical measurements

The performance of the anode made from cotton material in a zinc ion battery was evaluated using CR2032-type coin cells and a 2 M $ZnSO_4$ electrolyte solution. The cathode component, $(NH_4)_2V_{10}O_{25} \cdot 8H_2O$ (NVO), was synthesized following the procedures described in the available literature [31]. A cathode electrode made of NVO, with a weight of approximately 2.0 mg, was applied onto carbon paper using a slurry mixture consisting of NVO, conductive carbon, and PVDF at a ratio of 7:2:1. The configuration included the integration of polypropylene microporous separators (GF/D 47 mm). The diameter of both the cathode and anode electrodes was 14 mm. The NEWARE system was used to evaluate the performance of the Zn||Zn symmetric cell and Zn||NVO complete cell during charge-discharge cycling. An electrochemical workstation (CHI 660e, Chenhua, China) was used to conduct electrochemical evaluations, which included cyclic voltammetry (CV) and Tafel curve analysis.

3. Results and discussion

The cotton that underwent electroless nickel coating enables it to conduct electricity. We measured the electrical resistance, and the results are presented in Table 1.

The experiment was performed to measure the electrical resistance of conductive cotton that has undergone electroless nickel plating at a temperature of 50°C. We noticed time-based variations in physical characteristics. Figure 1(a) depicts the cotton in its original state, whereas Figure 1(b) illustrates the cotton after undergoing the electroless nickel plating process for 1 min to 3 min, resulting in the formation of nickel layers on its surface.

At nearly 5 min mark, there is a noticeable and erratic increase in the thickness of nickel layers on the fabric, leading to a resistance reading of 843 Ω, as depicted in Figure 1(c). After 7 min, a more consistent nickel coating has formed, resulting in a resistance measurement of 123 Ω (Figure 1(d)). Within a time frame of 9 min to 11 min, a fully formed layer of nickel becomes apparent, exhibiting resistance readings that are less than 15 Ω (Figure 1(e)). At around the 13 min point, the electroless reaction starts to decelerate, as seen by the appearance of a black solid. This indicates that the solution is running out and the process is nearing its end (Figure 1(f)).

As shown in the SEM images, cotton illustrates the fiber structure before electroless-nickel treatment (Figure 2(a-c). Upon undergoing electroless-nickel plating at 50°C for 9 min, nickel layers adhere to the surface (Figure 2(d-f)).

After 9 min of electroless-nickel treatment at 50°C, specimens underwent zinc electroplating at different current densities: 0.02 $A \cdot cm^{-2}$ for 60 min resulted in uneven zinc deposition, with less coverage at the center (Figure 3(a)). At 0.03 $A \cdot cm^{-2}$ for 40 min, a more uniform zinc layer was observed (Figure 3(b)). Finally, with 0.04 $A \cdot cm^{-2}$ for 30 min, zinc distribution was uniform, but more concentrated at the edges (Figure 3(c)).

As depicted in the SEM images, At 9 min of electroless-nickel treatment at 50°C zinc electroplating under different conditions is observed at a current density of 0.02 $A \cdot cm^{-2}$ for 60 min, a well-organized zinc layer adheres to the specimen surface, with minor gaps (Figure 4(a-c)). With a current density of 0.03 $A \cdot cm^{-2}$ for 40 min, the zinc layer adheres densely and uniformly to the structured specimen surface (Figure 4(d-f)). Lastly, at a current density of 0.04 $A \cdot cm^{-2}$ for 30 min, the zinc layer is distributed evenly across the specimen, though the deposition appears less orderly (Figure 4(g-i)).

Table 1. The electrical resistance of conductive cotton after electroless nickel plating.

Temperatures	**Time (min)**						
	1	**3**	**5**	**7**	**9**	**11**	**13**
40°C	N/A	N/A	N/A	N/A	930 Ω	670 Ω	340 Ω
50°C	N/A	N/A	843 Ω	123 Ω	15 Ω	8 Ω	Fail
60°C	N/A	962 Ω	186 Ω	Fail	Fail	Fail	Fail

The electrical resistance of conductive cotton is measured in Ω.

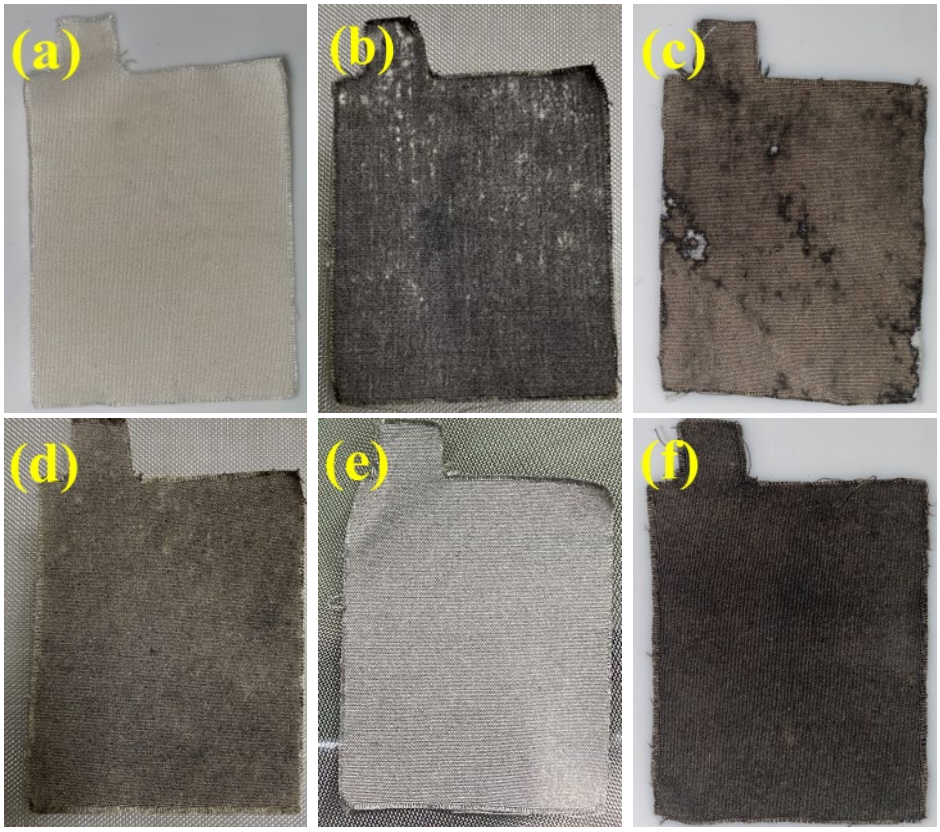

Figure 1. The physical characteristics of conductive cotton during the electroless nickel process at a temperature of 50°C, (a) The cotton before electroless nickel, (b) The cotton electroless-nickel process 1 min to 3 min, (c) Electroless-nickel process 5 min, (d) Electroless-nickel process 7 min, (e) Electroless-nickel process 9 min to 11 min, and (f) Electroless-nickel process after 13 min.

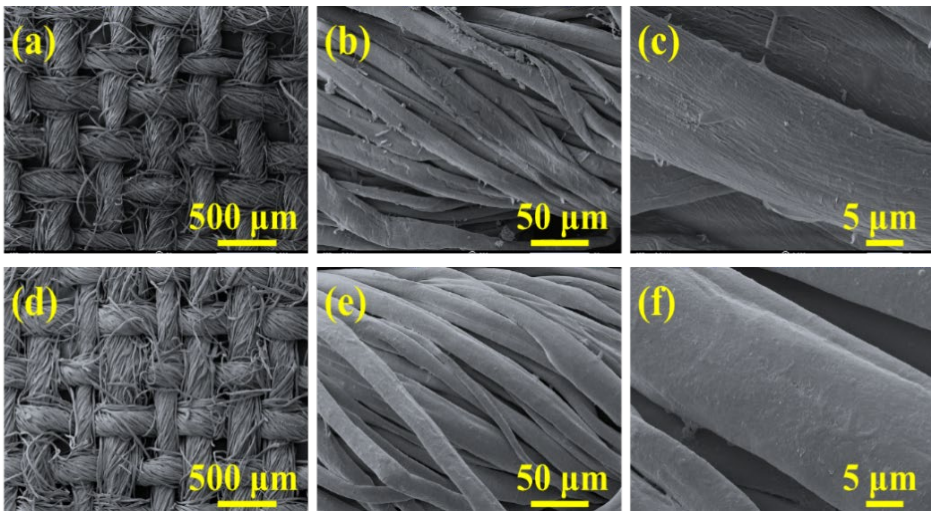

Figure 2. SEM images of cotton. (a) SEM of cotton before electroless-nickel ×50, (b) SEM of cotton before electroless-nickel ×500, (c) SEM of cotton before electroless-nickel ×3000, (d) SEM of cotton after electroless-nickel ×50, (e) SEM of cotton after electroless-nickel ×500, and (f) SEM of cotton after electroless-nickel ×3000.

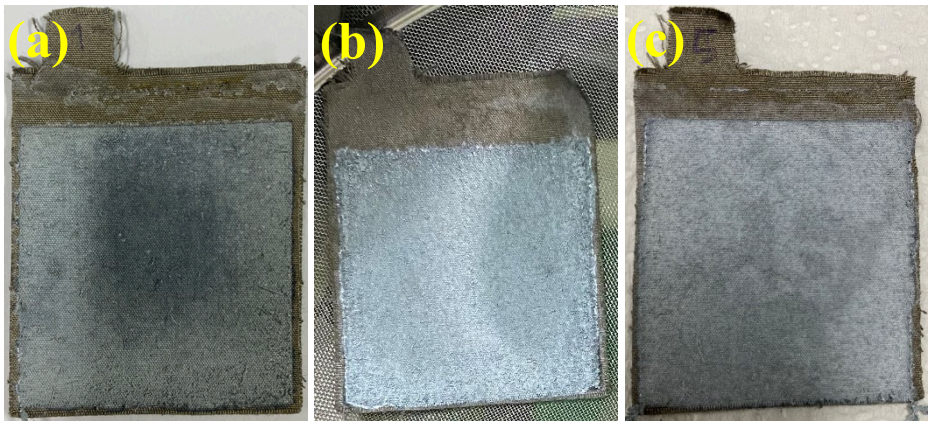

Figure 3. The images of physical characteristics of conductive cotton after the electroless nickel at a temperature of 50°C for 9 min and specimens underwent zinc electroplating, (a) Zinc electroplating at current densities: 0.02 A·cm^{-2} for 60 min, (b) Zinc electroplating at current densities: 0.03 A·cm^{-2} for 40 min, (c) Zinc electroplating at current densities: 0.04 A·cm^{-2} for 30 min.

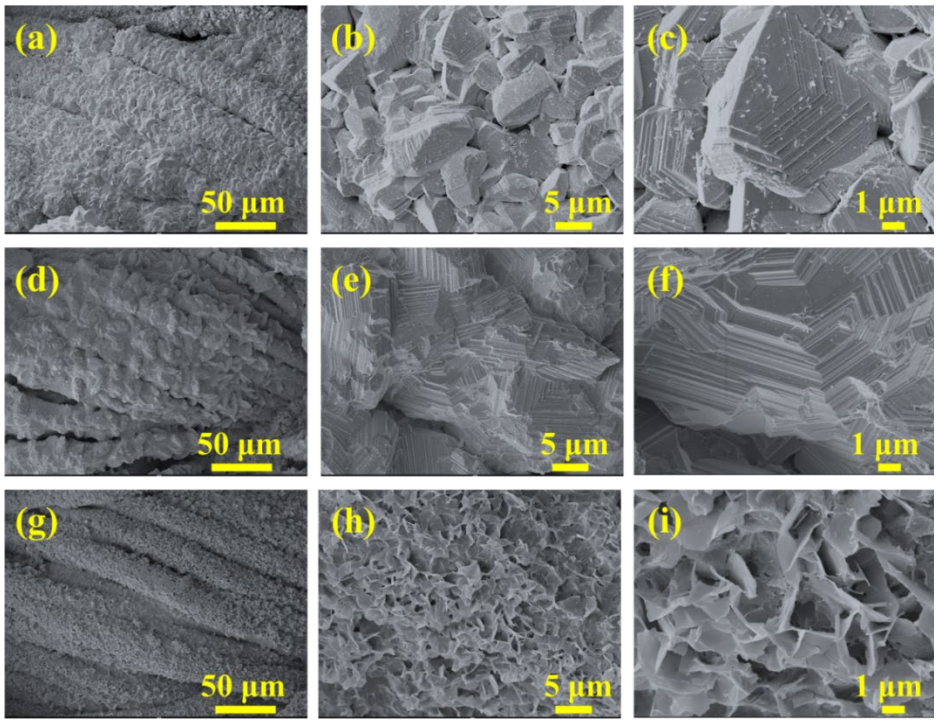

Figure 4. SEM images of conductive cotton after zinc electroplating, (a) SEM at a current density of 0.02 A·cm^{-2} for 60 min ×500, (b) SEM at a current density of 0.02 A·cm^{-2} for 60 min ×3000, (c) SEM at a current density of 0.02 A·cm^{-2} for 60 min ×10,000, (d) SEM at a current density of 0.03 A·cm^{-2} for 40 min ×500, (e) SEM at a current density of 0.03 A·cm^{-2} for 40 min ×3000, (f) SEM at a current density of 0.03 A·cm^{-2} for 40 min ×10000, (g) SEM at a current density of 0.04 A·cm^{-2} for 30 min ×500, (h) SEM at a current density of 0.04 A·cm^{-2} for 30 min ×3000, and (i) SEM at a current density of 0.04 A·cm^{-2} for 30 min ×10000.

In order to assess the efficiency of cotton treated with electroless nickel plating for a duration of 9 min at a temperature of 50°C, as an anode in a zinc-ion battery combined with a vanadium-based NVO cathode, we conducted tests on the Zn‖NVO battery at different levels of current density. Upon increasing the current density to 5 A·g^{-1}, we found a notable decrease in capacity. Furthermore, when the current density was reduced back to 0.1 A·g^{-1}, there was a considerable deterioration in capacity. In addition, we documented the subsequent capacity retentions during the process of zinc electroplating: 71.82% at a current density of 0.02 A·cm^{-2} for 60 min (Figure 5(a)), 74.69% at a current density of 0.03 A·cm^{-2} for 40 min (Figure 5(b)) and 70.92% at a current density of 0.04 A·cm^{-2} for 30 min (Figure 5(c)). The capacity retention data for all experiments, utilising electroless nickel plating for a duration of 7 min to 11 min at a temperature of 50°C, are succinctly presented in Table 2.

Based on the literature results we have crafted a comparative analysis table for zinc ion battery applications. Our findings align with the published literature about flexible zinc battery electrodes and their performance. As demonstrated in the aforementioned test results, illustrated in Table 3, our electrochemically deposited zinc ion battery attains a commensurate performance level.

The enhanced electrochemical activity and improved reversibility of chemical changes resulted in Zn‖NVO with a zinc-ion battery full cell anode made from cotton after undergoing 9 min of electroless-nickel treatment at 50°C, followed by electroplating at a current density of 0.03 A·cm^{-2} for 40 min. This configuration exhibited a discharge capacity of 132 mA·h·g^{-1} and capacity retention of 99.87% after 100 cycles at a current density of 2.1 A·cm^{-2}.

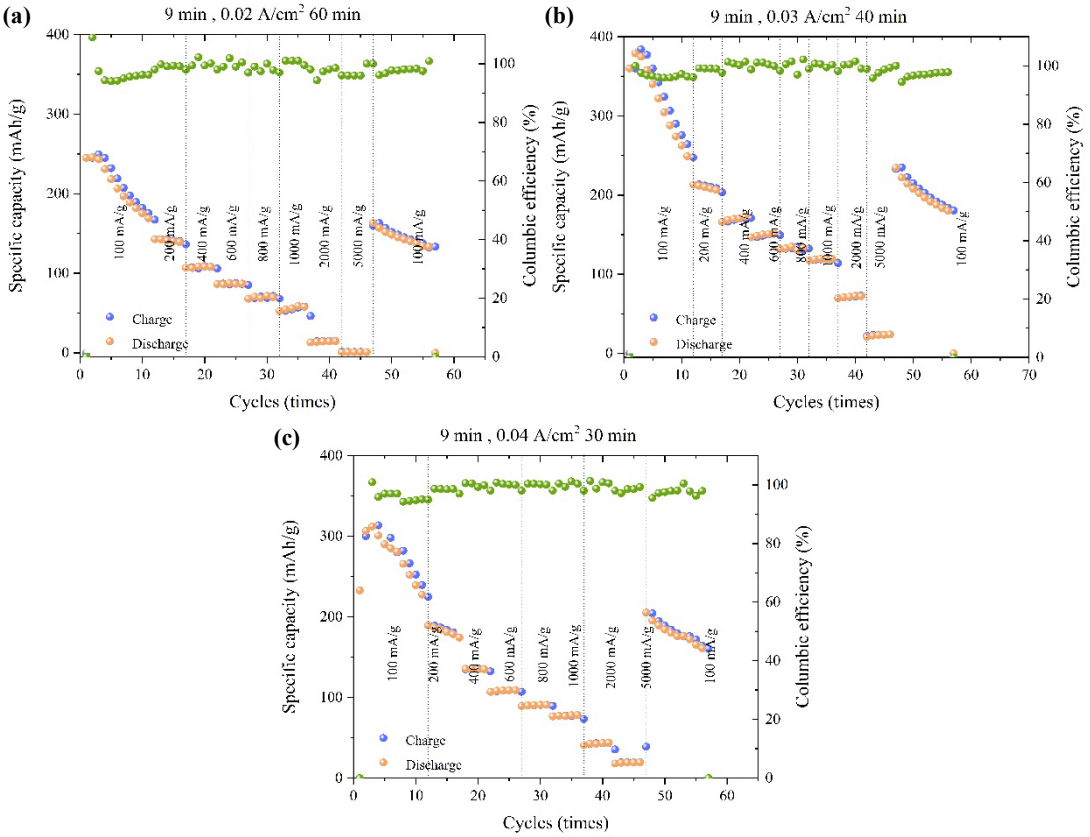

Figure 5. Electrochemical performance of Zn‖NVO full cells with 9 min of electroless-nickel treatment at 50°C, (a) A current density of 0.02 A·cm^{-2} for 60 min of zinc electroplating, (b) A current density of 0.03 A·cm^{-2} for 40 min of zinc electroplating, and (c) A current density of 0.04 A·cm^{-2} for 30 min of zinc electroplating.

Table 2. The corresponding values for capacity retention and discharge capacity, summarizing the electrochemical performance of Zn‖NVO full cells, are presented.

Time electroless nickel at 50 °C (min)	Current densities type	Discharge capacity (mA·h·g^{-1})	Capacity retention (%)
7	0.02 A·cm^{-2} for 60 min	106.39	0.018
	0.03 A·cm^{-2} for 40 min	174.55	40.68
	0.04 A·cm^{-2} for 30 min	126.87	46.11
9	0.02 A·cm^{-2} for 60 min	181.74	71.82
	0.03 A·cm^{-2} for 40 min	249.19	74.69
	0.04 A·cm^{-2} for 30 min	227.52	70.92
11	0.02 A·cm^{-2} for 60 min	166.97	65.65
	0.03 A·cm^{-2} for 40 min	249.25	73.78
	0.04 A·cm^{-2} for 30 min	196.97	73.52

Table 3. Comparison Performance Metrics for Flexible Zinc-Ion Batteries.

Anode	Cathode	Specific capacity (mA·h·g^{-1})	Ref.
Zinc-plated on cotton	$(NH_4)_2V_{10}O_{25}·8H_2O$ (NVOD)	249.19 at 0.1 A·g^{-1}	This work
Electrodepositing Zn metal on carbon cloth	h-VOW	455 at 0.1 A·g^{-1}	[32]
Electrochemically depositing zinc metal nanosheets	MnO_2	300.4 at 0.11 A·g^{-1}	33]
Electroplated Zn on carbon cloth	MnO_2	332.2 at 0.3 A·g^{-1}	[34]
Zinc electrodeposition method	MnO_2	289 at 0.1 A·g^{-1}	[35]
Zinc NPs uniformly deposited onto N-CC	MnO_2	353 at 0.5 A·g^{-1}	[36]

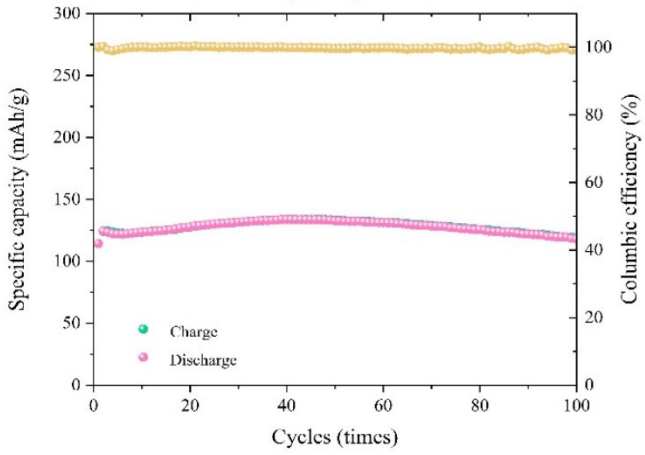

Figure 6. Long-term cycling performance of the Zn‖NVO with zinc anode on nickel conductive cloth.

To assess the effectiveness of the zinc-ion battery, which was developed using cotton treated with electroless nickel for 9 min at a temperature of 50°C, in enhancing the stability and reversibility of Zn electrodes, we carried out a comparison of the long-term charge-discharge cycling performance of Zn‖Zn symmetric cells utilizing separators. The symmetric cells with Zn‖Zn configuration, when evaluated at a current intensity of 0.5 mA·cm^{-2}, exhibited a significantly extended cycle lifespan of 1000 h, as shown in Figure 7(a). Figure 7(b) displays the EIS plots for the symmetric cell with the fitted equivalent circuit, which features two semicircular arcs indicating resistance associated with the cell. The semicircle's diameter at the highest frequency is commonly attributed to (i) electrode resistance, (ii) charge transfer resistance linked to pseudocapacitive charge storage involving redox reactions and/or ion intercalation, or (iii) resistance of the electrolyte on a porous electrode. The Rs value, representing the electrolyte solution resistance, is obtained from the intercept of the plot at the high-frequency region on the real axis (X-axis). For both the obtained and fitted plots, this value is approximately 1.5 Ω. The Rct value, indicating the charge transfer resistance, is derived from the diameter of the semicircle at the high-frequency region. The Rct is approximately 16 Ω and 13 Ω for the obtained and fitted equivalent circuit values. Thus, the EIS analysis demonstrates that using a zinc anode on nickel conductive cloth can reduce the charge transfer resistance (Rct) compared to other materials, indicating potential improvements in efficiency and stability for long-term zinc ion battery applications. Figure 7(c) presents the CV curves at a scan rate of 0.1 mV·s^{-1}. Hence, the above results conclude the use of a zinc anode on nickel conductive cloth for zinc-ion battery applications exhibits potential for battery manufacturing and further advancement.

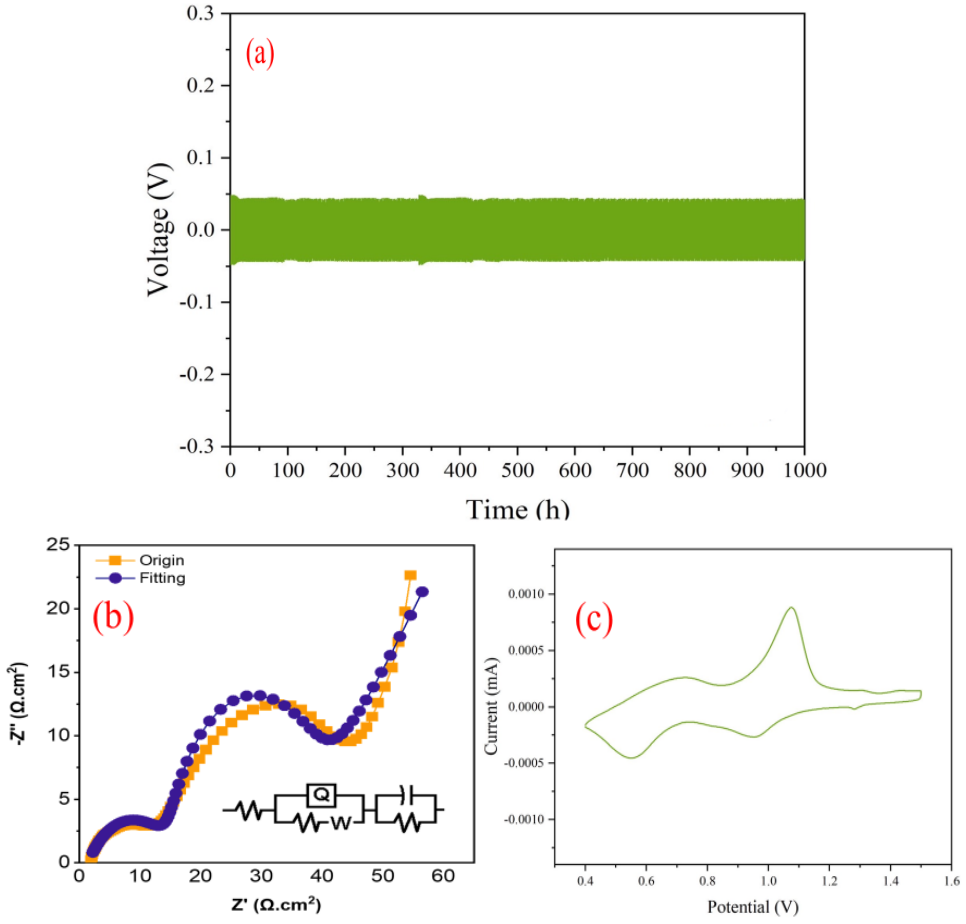

Figure 7. Electrochemical performance of Zn‖Zn symmetric with zinc anode on nickel conductive cloth, (a) Charge−discharge cycling performances 0.5 mA·cm^{-2}, (b) EIS plots of Zn‖Zn symmetric with zinc anode on nickel conductive cloth, and (c) CV curves at the scan rate of 0.1 mV·s^{-1}.

4. Conclusions

In summary, a zinc anode on nickel conductive cloth for zinc-ion battery applications was prepared using electroless nickel plating on conductive cotton. Under the condition of 9 min of electroless-nickel treatment at 50°C, the electrical resistance was 15 Ω, while 11 min of electroless-nickel treatment at 50°C resulted in a resistance of 8 Ω. Since the zinc electroplating tests yielded similar results, the 9 min treatment was chosen for its shorter preparation time. The Zn‖NVO full cell with a zinc anode on nickel conductive cloth exhibited high cycling capacity and stability, with a discharge capacity of 249.19 $mA{\cdot}h{\cdot}g^{-1}$ and capacity retention of 74.69% after 60 cycles at 1 $A{\cdot}g^{-1}$. Long-term cycling performance showed a discharge capacity of 132 $mA{\cdot}h{\cdot}g^{-1}$ and a capacity retention of 99.87% after 100 cycles at a current density of 2.1 $A{\cdot}cm^{-2}$. The Zn‖Zn symmetric cells initially tested at a current density of 0.5 $mA{\cdot}cm^{-2}$ demonstrated a prolonged cycling lifespan of 1000 h. Therefore, using a zinc anode on nickel conductive cloth for zinc-ion battery applications holds promise for battery production and future development. This method offers advantages such as easy manufacturing, low cost, and high efficiency, making it an excellent choice for creating flexible batteries.

Acknowledgment

This work is supported by the National Science, Research, and Innovation Fund (NSRF) via the Program Management Unit for Human Resources & Institutional Development, Research, and Innovation (Grant No. B16F640190). M. K would like to thank Chulalongkorn University in Thailand for their C2F scholarship sponsorship. J. Q. thanks the National Research Council of Thailand (NRCT) and Chulalongkorn University (N42A660383).

References

[1] A. Ali Ahmed, A. Alsharif, and Y. Nassar, "Recent Advances in Energy Storage Technologies," *Energy Storage*, vol. 1, pp. 9-17, 2023.

[2] M. Shetty, K. Manickavasakam, C. Sabbanahalli, C. Bekal, I. I. Misnon, S. Subrahmanya, K. Roy, P. D. Shivaramu, S. Shenoy p, and D. Rangappa, "Rapid single pot synthesis of hierarchical Bi_2WO_6 microspheres/RGO nanocomposite and its application in energy storage: A supercritical water approach," *Journal of Energy Storage,* vol. 72, Part B, p. 108116, 2023.

[3] D. Rangappa, K. Manickavasakam, M. Muniyappa, C. Bekal, S. Shenoy B, I. I. Misnon, M. Kandasamy, and M. Shetty. "A rapid supercritical water approach for one-pot synthesis of a branched $BiVO_4$/RGO composite as a Li-ion battery anode," *RSC Advances,* vol. 14, no. 11, pp. 7699-7709, 2024.

[4] N. Apparla, K. Manickavasakam, and C. S. Sharma, "Augmenting the supercapacitive performance of candle soot-derived activated carbon electrodes in aqueous and non-aqueous electrolytes," *Journal of Energy Storage,* vol. 73, p. 109162, 2023.

[5] R. Samantray, K. Manickavasakam, Vivekanand, B. Pradhan, M. Kandasamy, S. C. Mishra, I. I. Misnon, and R. Jose, "Nanoarchitectonics of low process parameter synthesized porous carbon on enhanced performance with synergistic interaction of redox-active electrolyte for supercapacitor application," *Materials Chemistry and Physics,* vol. 314, p. 128885, 2024.

[6] A. Godfrey, V. Hetherington, H. Shum, P. Bonato, N. H. Lovell, and S. Stuart, "From A to Z: Wearable technology explained," (in eng), *Maturitas,* vol. 113, pp. 40-47, 2018.

[7] Y. F. Yuan, J. Tu, H. M. Wu, B. Zhang, X. H. Huang, and X. B. Zhao, "Preparation, characteristics and electrochemical performance of $Sn_6O_4(OH)_4$-coated ZnO for Zn–Ni secondary battery," *Electrochemistry Communications,* vol. 8, pp. 653-657, 2006.

[8] S. -H. Lee, C. -W. Yi, and K. Kim, "Characteristics and "Electrochemical Performance of the TiO_2-Coated ZnO anode for Ni−Zn secondary batteries," *The Journal of Physical Chemistry C,* vol. 115, pp. 2572-2577, 2010.

[9] J. F. Parker, C. N. Chervin, I. R. Pala, M. Machler, M. F. Burz, J. W. Long, D. R. Folison, "Rechargeable nickel-3D zinc batteries: An energy-dense, safer alternative to lithium-ion," (in eng), *Science,* vol. 356, no. 6336, pp. 415-418, 2017.

[10] S. S. Hosseiny, and M. Wessling, "13 - Ion exchange membranes for vanadium redox flow batteries," in *Advanced Membrane Science and Technology for Sustainable Energy and Environmental Applications*, A. Basile and S. P. Nunes Eds.: Woodhead Publishing, 2011, pp. 413-434.

[11] "Chapter 4 - Primary Batteries," in *Batteries for Portable Devices*, G. Pistoia Ed. Amsterdam: Elsevier Science B.V., 2005, pp. 33-76.

[12] F. R. McLarnon, and E. J. Cairns, "The Secondary alkaline zinc electrode," *Journal of The Electrochemical Society,* vol. 138, no. 2, p. 645, 1991.

[13] P. Simon, Y. Gogotsi, and B. Dunn, "Materials science. where do batteries end and supercapacitors begin?," (in eng), *Science,* vol. 343, no. 6176, pp. 1210-1211, 2014.

[14] F. R. Mclarnon, and E. J. Cairns, "The secondary alkaline zinc electrode," *Journal of The Electrochemical Society,* vol. 138, pp. 645-664, 1991.

[15] E. Frąckowiak, and J. M. Skowroński, "Passivation of zinc in alkaline solution effected by chromates and CrO_3–graphite system," *Journal of Power Sources,* vol. 73, no. 2, pp. 175-181, 1998.

[16] D. G. Mackanic, T. H. Chang, Z. Huang, Y. Cui, and Z. Bao, "Stretchable electrochemical energy storage devices," (in eng), *Chemical Society Reviews Journal,* vol. 49, no. 13, pp. 4466-4495, 2020.

[17] Z. Liu, F. Mo. H. Li, M. Zhu, Z. Wang, G. Liang, and C. Zhi, "Advances in flexible and wearable energy-storage textiles," *Small Methods,* vol. 2, 2018.

[18] L. Hu, H. Wu, F. La Mantia, Y. Yang, and Y. Cui, "Thin, flexible secondary Li-ion paper batteries," (in eng), *ACS Nano,* vol. 4, no. 10, pp. 5843-5848, 2010.

[19] D. Chen, Z. Lou, K. Jiang, and G. Shen, "Device configurations and future prospects of flexible/stretchable lithium-ion batteries," *Advanced Functional Materials,* vol. 28, 2018.

[20] W.-w. Liu, X.-b. Yan, J.-w. Lang, C. Peng, and Q.-j. Xue, "Flexible and conductive nanocomposite electrode based on graphene sheets and cotton cloth for supercapacitor," *Journal of Materials Chemistry,* 10.1039/C2JM32659K vol. 22, no. 33, pp. 17245-17253, 2012.

[21] C. Zhang, G. Zhou, W. Rao, L. Fan, W. Xu, and J. Xu, "A simple method of fabricating nickel-coated cotton fabrics for wearable strain sensor," *Cellulose,* vol. 25, no. 8, pp. 4859-4870, 2018.

[22] G. G. Gavrilov, *Chemical (electroless) Nickel-plating*. Portcullis Press, 1979.

[23] G. O. Mallory, J. B. Hajdu, A. Electroplaters, and S. F. Society, *Electroless Plating: Fundamentals and Applications*. The Society, 1990.

[24] S. Furukawa, and M. Mehregany, "Electroless plating of nickel on silicon for fabrication of high-aspect-ratio microstructures," *Sensors and Actuators A: Physical,* vol. 56, no. 3, pp. 261-266, 1996.

[25] S. Olivera, H. B. Muralidhara,nK. Venkatesh, K. Gopalakrishna, S. S. Vivek, "Plating on acrylonitrile–butadiene–styrene (ABS) plastic: a review," *Journal of Materials Science,* vol. 51, no. 8, pp. 3657-3674, 2016.

[26] J. D. Moore, "Acrylonitrile-butadiene-styrene (ABS) - A review," *Composites,* vol. 4, no. 3, pp. 118-130, 1973.

[27] S. Ghosh, "Electroless copper deposition: A critical review," *Thin Solid Films,* vol. 669, pp. 641-658, 2019.

[28] Y. Boonyongmaneerat, V. Srisupornwichai, C. Aumnate, P. Visuttipitukul, S. T. Dubas, M. Metzner, and M. Zinn, "Strategies for metallizing and electroplating biodegradable PLA," *Current Applied Science and Technology,* vol. 22, no. 3, 2021.

[29] K. Lolupiman, P. Wangyao, and J. Qin, "Electrodeposition of Zn/TiO_2 composite coatings for anode materials of Zinc ion battery," *Journal of Metals, Materials and Minerals,* vol. 29, no. 4, 2019.

[30] J. Cao, D. Zhang, X. Zhang, M. Sawangphruk, J. Qin, and R. Liu, "A universal and facile approach to suppress dendrite formation for a Zn and Li metal anode," *Journal of Materials Chemistry A,* 10.1039/D0TA02486D vol. 8, no. 18, pp. 9331-9344, 2020.

[31] J. Cao, D. Zhang, Y. Yue, X. Wang, T. Pakornchote, T. Bovornratanaraks, X. Zhang, Z-S. Wu, and J. Qin, "Oxygen defect enriched $(NH_4)_2V_{10}O_{25}\cdot 8H_2O$ nanosheets for superior aqueous zinc-ion batteries," *Nano Energy,* vol. 84, p. 105876, 2021.

[32] X. Li, L. Ma, Y. Zhao, Q. Yang, D. Wang, Z. Huang, G. Liang, F. Mo. Z. Liu, and C. Zhi, "Hydrated hybrid vanadium oxide nanowires as the superior cathode for aqueous Zn battery," *Materials Today Energy,* vol. 14, p. 100361, 2019.

[33] Z. Liu, D. Wang, Z. Tang, G. Liang, Q. Yang, H. Li, L. Ma, F. Mo. and C. Zhi, "A mechanically durable and device-level tough Zn-MnO_2 battery with high flexibility," *Energy Storage Materials,* vol. 23, pp. 636-645, 2019.

[34] Y. Huang, J. Liu, Q. Huang, Z. Zheng, P. Hiralal, F. Zheng, D. Ozgit, S. Su, S. Chen, P-H. Tan, S. Zhang, and H. Zhou, "Flexible high energy density zinc-ion batteries enabled by binder-free MnO_2/reduced graphene oxide electrode," *npj Flexible Electronics,* vol. 2, no. 1, 2018.

[35] Y. Zeng, X. Zhang, R. Qin, X. Liu, P. Fang, D. Zheng, Y. Tong, and X. Lu, "Dendrite-free zinc deposition induced by multi-functional CNT frameworks for stable flexible Zn-Ion batteries," *Advanced Materials,* vol. 31, p. 1903675, 2019.

[36] Q. Wenda, Y. Li, A. You, Z. Zhang, G. Li, X. Lu, and Y. Tong, "High-performance flexible quasi-solid-state Zn-MnO_2 battery based on MnO_2 nanorod arrays coated 3D porous nitrogen-doped carbon cloth," *Journal of Materials Chemistry A.,* vol. 5, 2017.